Molecular Cell, Vol. 16, 35–45, October 8, 2004, Copyright ©2004 by Cell Press

# GSK3-Mediated BCL-3 Phosphorylation Modulates Its Degradation and Its Oncogenicity

**Patrick Viatour,[1] Emmanuel Dejardin,[4] Michael Warnier,[1] Florence Lair,[1] Estefania Claudio,[5] Fabrice Bureau,[2] Jean-Christophe Marine,[6] Marie-Paule Merville,[1] Ulrich Maurer,[4] Douglas Green,[4] Jacques Piette,[3] Ulrich Siebenlist,[5] Vincent Bours,[1] and Alain Chariot[1,*]**

[1]Laboratory of Medical Chemistry and Human Genetics
[2]Department of Physiology
[3]Laboratory of Virology and Immunology
Center for Biomedical Integrated Genoproteomics
University of Liège, Sart-Tilman
4000 Liège
Belgium
[4]Division of Cellular Immunology
La Jolla Institute for Allergy and Immunology
San Diego, California 92121
[5]Laboratory of Immunoregulation
National Institute of Allergy and Infectious Diseases
National Institutes of Health
Bethesda, Maryland 20892
[6]Laboratory for Molecular Cancer Biology
Flanders Interuniversity Institute for Biotechnology
Ghent
Belgium

## Summary

**The oncoprotein BCL-3 is a nuclear transcription factor that activates NF-κB target genes through formation of heterocomplexes with p50 or p52. BCL-3 is phosphorylated in vivo, but specific BCL-3 kinases have not been identified so far. In this report, we show that BCL-3 is a substrate for the protein kinase GSK3 and that GSK3-mediated BCL-3 phosphorylation, which is inhibited by Akt activation, targets its degradation through the proteasome pathway. This phosphorylation modulates its association with HDAC1, -3, and -6 and attenuates its oncogenicity by selectively controlling the expression of a subset of newly identified target genes such as *SLPI* and *Cxcl1*. Our results therefore suggest that constitutive BCL-3 phosphorylation by GSK3 regulates BCL-3 turnover and transcriptional activity.**

## Introduction

Constitutive NF-κB activation, a hallmark of many human cancers, upregulates the expression of antiapoptotic genes and therefore disrupts the balance between apoptosis and proliferation (Karin et al., 2002). In some cases, high NF-κB activity in cancer cells results from point mutations or translocations of the genes coding for the NF-κB or IκB proteins, whereas in other cases, mutations have not been described, despite high IKK and NF-κB activities (Karin et al., 2002). The BCL-3 protein is a member of the IκB family of NF-κB inhibitors and was originally identified through molecular cloning of the breakpoint of the t(14;19) chromosome translocation from a subset of human B cell chronic lymphotic leukemias (McKeithan et al., 1987). This translocation causes BCL-3 overexpression and presumably dysregulation of still mostly unknown downstream target genes involved in cell proliferation and differentiation (Ohno et al., 1990). BCL-3 is also expressed in human breast tumors (Cogswell et al., 2000) with deregulated cyclin D1 expression, suggesting that *cyclin D1* may be one of the few BCL-3 target genes identified (Westerheide et al., 2001). However, evidence for BCL-3-induced transformation is missing.

BCL-3 is constitutively phosphorylated in vivo (Fujita et al., 1993; Nolan et al., 1993; Bundy and McKeithan, 1997), but the kinase(s) responsible for BCL-3 phosphorylation in vivo remain(s) to be identified.

We show here that BCL-3 is phosphorylated by GSK3 and subsequently degraded through the proteasome pathway. This BCL-3 phosphorylation modulates its oncogenic potential in vitro and in vivo and regulates the expression of a subset of newly identified BCL-3 target genes. Taken together, our results suggest that constitutive BCL-3 phosphorylation by GSK3 prevents its cellular accumulation and inhibits its oncogenic potential.

## Results

### GSK3β Phosphorylates BCL-3

In the process of studying BCL-3 expression in leukemia, we detected multiple forms of the BCL-3 protein in several leukemic samples, therefore suggesting post-translational modifications such as phosphorylation (Viatour et al., 2003a). Because no BCL-3 kinase has been identified so far, we searched for potential candidates by first mapping the BCL-3 targeted domain. 293 cells were transfected with expression plasmids coding for FLAG-tagged wild-type BCL-3, ΔC BCL-3, ΔN BCL-3, or a BCL-3 protein harboring only the ankyrin repeats (Figure 1A, lanes 2, 3, 4, and 5, respectively), and cell extracts were subjected to anti-FLAG Western analysis. Slower migrating forms were detectable for the wild-type BCL-3 protein as well as for ΔN BCL-3 (Figure 1A, lanes 2 and 4), but not for the other BCL-3 mutants (Figure 1A, lanes 3 and 5). To demonstrate that these slower migrating forms are due to phosphorylation, 10 or 20 μl of cell extracts from 293 cells transfected with FLAG-BCL-3 was left untreated (Figure 1B, lanes 2 and 4) or incubated with λ phosphatase (Figure 1B, lanes 3 and 5). Using both amounts of cell extracts, we observed that the phosphatase treatement led to the disappearance of the slower migrating BCL-3 forms (Figure 1B, compare lanes 2 and 4 with lanes 3 and 5).

To search for BCL-3 kinase, in silico analysis was carried out using the Scansite software (see Experimental Procedures). The kinase-accessible surface essentially lies at the C-terminal end of the protein, in agreement with the results described in Figure 1A (data not shown). Several putative phosphorylation sites were

*Correspondence: alain.chariot@ulg.ac.be

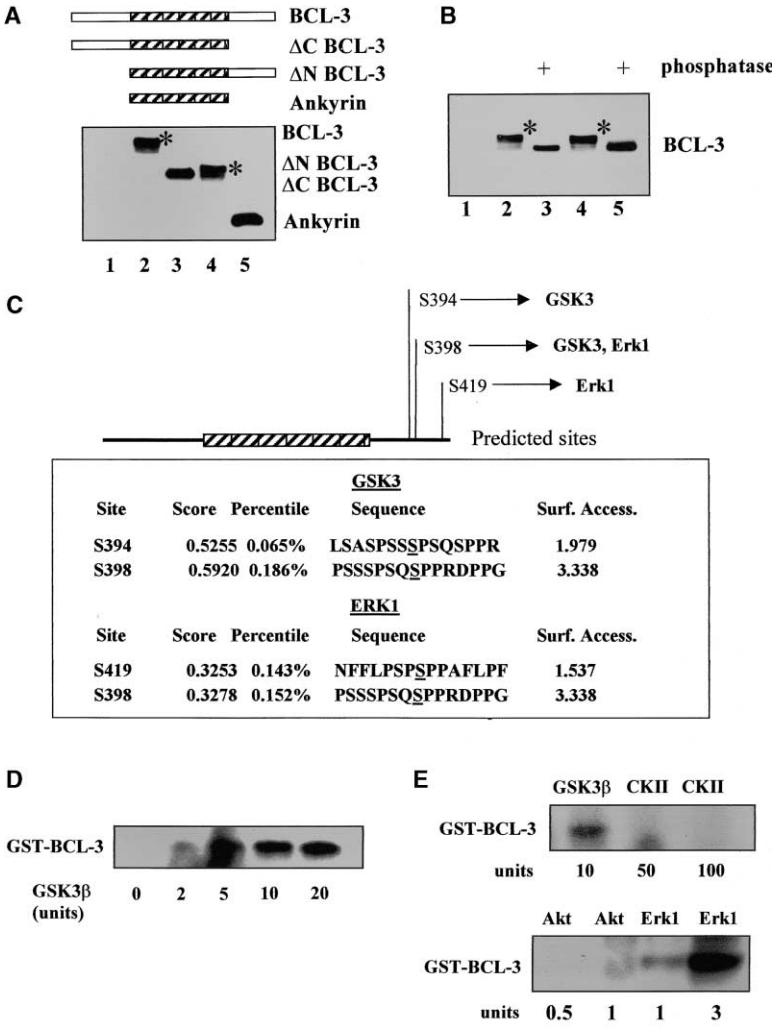


Figure 1. BCL-3 Phosphorylation by GSK3 In Vitro

(A) BCL-3 is phosphorylated downstream of the ankyrin repeats. (Top) Representation of the wild-type BCL-3 protein and the BCL-3 mutants. Anti-FLAG Western blots were carried out on extracts from 293 cells transfected with pcDNA3 alone (lane 1) or with the indicated FLAG-tagged wild-type (lane 2) and BCL-3 mutant expression vectors (ΔC BCL-3, ΔN BCL-3, and ankyrin domain in lanes 3, 4, and 5, respectively). The asterisks illustrate the phosphorylated form of BCL-3.

(B) λ phosphatase dephosphorylates ectopically expressed FLAG-BCL-3. 293 cells were transfected with an empty vector (lane 1) or with FLAG-BCL-3 (lanes 2–5). 10 (lanes 2 and 3) or 20 μl (lanes 4 and 5) of extracts were untreated (lanes 2 and 4) or incubated with 400 units of phosphatase (lanes 3 and 5) at 37°C for 1 hr and subsequently subjected to anti-FLAG Western analysis.

(C) Representation of the BCL-3 protein. The ankyrin repeats (aa 126–329) are shown as hatched rectangles. The putative BCL-3 kinases and phosphorylated sites as well as the percentile values are mentioned.

(D and E) BCL-3 is phosphorylated by GSK3 and Erk1 but not by Akt nor CKII in vitro. A purified GST-BCL-3 fusion protein was incubated with increasing amounts of recombinant GSK3β (D) or active Akt, Erk1, or CKII (E), and in vitro kinase assays were done.

identified on BCL-3 and included two Erk1 sites as well as two distinct GSK3-target residues at S394 and S398 (Figure 1C, top panel). Therefore, BCL-3 is phosphorylated on its C-terminal domain, downstream of the ankyrin repeats, as previously suggested (Bundy and McKeithan, 1997).

To determine whether BCL-3 is phosphorylated by GSK3, recombinant GSK3β kinase was incubated with purified GST-BCL-3 protein. A strong dose-dependent signal was detected (Figure 1D). Because phosphorylation by GSK3 needs to be primed by a prior phosphorylation mediated by another kinase, in most cases CKII, we investigated whether this latter kinase phosphorylates BCL-3 in vitro by incubating either a GSK3β (positive control) or a CKII recombinant protein with a GST-BCL-3 fusion protein. We did not detect any BCL-3 phosphorylation by CKII (Figure 1E, top panel). Moreover, the kinase Akt, which is known to phosphorylate and to inhibit GSK3, did not phosphorylate BCL-3 in vitro, whereas Erk1 did (Figure 1E, lower panel).

We transfected 293 cells with a GSK3β expression vector and performed either an anti-HA (negative control) or an anti-GSK3β immunoprecipitation, and the resulting immunoprecipitates were used for an in vitro kinase assay with a purified GST-BCL-3 protein as a substrate (Figure 2A). Again, a BCL-3 phosphorylation was detected with the anti-GSK3β, but not with the anti-HA, immunoprecipitates (Figure 2A).

To further demonstrate that GSK3 phosphorylates BCL-3, 293 cells were transfected with an empty vector or FLAG-BCL-3 (Figure 2B, left panels, lanes 1 and 2–5, respectively) and subsequently left untreated (Figure 2B, left panels, lanes 1 and 2) or incubated with increasing concentrations of LiCl, a specific GSK3 inhibitor (Figure 2B, left panels, lanes 3–5). Anti-FLAG Western analysis performed on the cell extracts indicated that LiCl treatment led to a dose-dependent decrease of the BCL-3 slower migrating forms with increased expression levels of the BCL-3 hypophosphorylated proteins (Figure 2B, left upper panel, compare lanes 3–5 with lane 2). Moreover, when 293 cells were transfected with an expression vector coding for a BCL3 mutant lacking both GSK3 phosphorylation sites (S394 and S398, and named "BCL-3 MT S") and treated with LiCl, this inhibitor had no effect on the BCL-3 MT S migration profile (Figure 2B, right upper panel, compare lanes 2 and 3). Similarly, exogenous expression of GSK3β did not modify the BCL-3 MTS migration profile (lane 4). To investigate the effect of

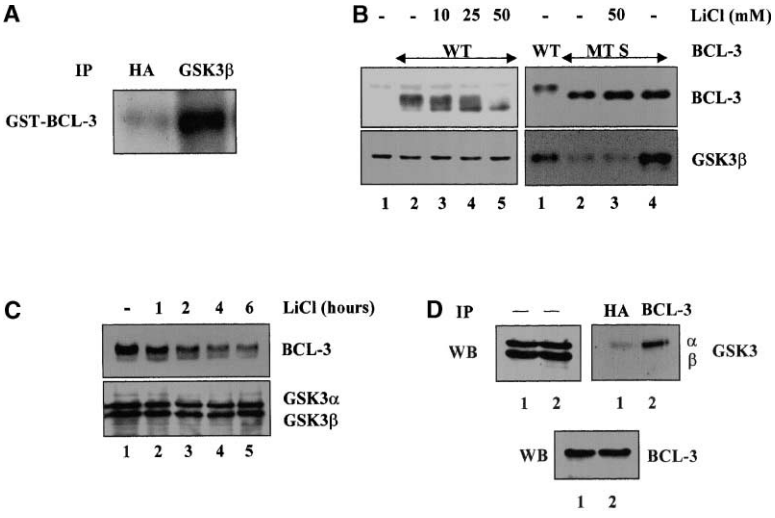


Figure 2. BCL-3 Is Phosphorylated by GSK3

(A) GSK3-mediated BCL-3 phosphorylation in 293 cells. Anti-HA (negative controls) or anti-GSK3β immunoprecipitates from 293 cells transfected with a GSK3β expression vector were subjected to an in vitro kinase assay using a purified GST-BCL-3 protein as substrate.

(B and C) LiCl inhibits GSK3-mediated BCL-3 phosphorylation. (B) 293 cells were transfected with pcDNA3 (left panels, lane 1), wild-type FLAG-BCL-3 (left panels, lanes 2–5, and right panels, lane 1), FLAG BCL-3 MT S (right panels, lanes 2–4), and with GSK3β (right panels, lane 4) and were left unstimulated (left panels, lanes 1 and 2, and right panels, lanes 1, 2, and 4) or treated with increasing concentrations of LiCl, as indicated. Extracts were subjected to anti-FLAG or GSK3β Western blots (top and bottom panels, respectively). (C) Karpas cells were left untreated (lane 1) or incubated with LiCl for the indicated periods of time (lanes 2–5). Cell extracts were subjected to anti-BCL-3 and GSK3α/β Western analysis.

(D) Endogenous BCL-3 and GSK3α proteins interact. Karpas cell extracts were immunoprecipitated with anti-HA or BCL-3 antibodies (lanes 1 and 2, respectively), and an anti-GSK3 Western blot was performed on the immunoprecipitates (top right panel). Extracts were subjected to anti-GSK3 (top left panel) and BCL-3 Western analysis (bottom panel).

LiCl on endogenous BCL-3, we selected the Karpas cell line, which highly expresses BCL-3 (Nishikori et al., 2003). These cells were left untreated or stimulated from 1 to 6 hr with LiCl, and the status of GSK3-mediated BCL-3 phosphorylation was assessed by Western analysis (Figure 2C). BCL-3 appeared mostly hyperphosphorylated in unstimulated cells (Figure 2C, upper panel, lane 1), but LiCl treatment led to severe decrease of the BCL-3 phosphorylated forms, whereas the BCL-3 hypophosphorylated forms remained unchanged (Figure 2C, upper panel, compare lane 1 with lanes 2–5). Taken together, these results indicate that GSK3 phosphorylates BCL-3. The ability of GSK3 to interact with BCL-3 was investigated by coimmunoprecipitation experiments in Karpas cells. Endogenous GSK3α, but not GSK3β, was found in anti-BCL-3, but not in anti-HA, immunoprecipitates (Figure 2D, top right panel, lanes 2 and 1, respectively). Therefore, GSK3 interacts and phosphorylates BCL-3 on S394 and S398.

### GSK3-Mediated Phosphorylation Targets BCL-3 Degradation

BCL-3 is a nuclear protein, unlike the other members of the IκB family. To determine whether GSK3-mediated BCL-3 phosphorylation regulates its cellular localization as described for cyclin D1 (Diehl et al., 1998), BCL-3 wild-type or MT S was expressed in 293 cells, and immunofluorescence experiments showed that both ectopically expressed proteins were found in the nucleus (data not shown). Therefore, GSK3-mediated phosphorylation does not regulate BCL-3 cellular localization.

Because GSK3-mediated phosphorylation triggers subsequent proteolysis of the substrate (Diehl et al., 1998; Welcker et al., 2003), we investigated whether BCL-3 stability was modulated by GSK3 phosphorylation. 293 cells were transfected either with the wild-type or MT S BCL-3 expression plasmids and subsequently treated with cycloheximide (CHX). Wild-type BCL-3 protein levels decreased after 2 hr of treatment of CHX whereas BCL-3 MT S remained stable up to 4 hr of treatment (Figure 3A), suggesting that GSK3-mediated phosphorylation triggers BCL-3 degradation.

To determine whether BCL-3 is degraded through the proteasome pathway, we assessed BCL-3 stability in the presence of MG132, a proteasome inhibitor. 293 cells were transfected with a BCL-3 expression plasmid and left unstimulated or treated with CHX and/or MG132 (Figure 3B). BCL-3 proteins were barely detectable after 4 hr of CHX treatment, as shown before (Figure 3B, third lane), but pretreatment with MG132 prevented BCL-3 degradation (Figure 3B, upper panel, fourth lane). We also noticed that MG132 alone enhanced BCL-3 expression (Figure 3B, upper panel, fifth lane), confirming that BCL-3 degradation occurs through the proteasome.

Because proteasome-mediated degradation follows protein ubiquitination on the lysine ϵ amino group (Ben-Neriah, 2002), we determined whether GSK3 triggers BCL-3 polyubiquitin linkage. 293 cells were transfected with expression vectors coding for HA-ubiquitin and FLAG-BCL-3 with or without increasing amounts of a GSK3β expression vector. Cells were treated with MG132 for 90 min, and anti-FLAG immunoprecipitations followed by anti-HA Western analysis were carried out. GSK3β dose-dependent ubiquitin-conjugated BCL-3 adducts were detected in cells overexpressing both FLAG-BCL-3 and GSK3β (Figure 3C, top panel, lanes 3 and 4), suggesting that this kinase indeed triggers BCL-3 polyubiquitination. To determine whether LiCl affected GSK3-mediated BCL-3 ubiquitination, 293 cells were transfected with expression vectors for HA-Ub (Figure 3D, lanes 1–5), FLAG-BCL-3 (lanes 2–5), and GSK3 (lanes 4 and 5) and subsequently treated with LiCl, as indicated (lanes 3 and 5), followed by a 2 hr stimulation with MG132 (lanes 1–5). Anti-FLAG immunoprecipitations followed by anti-HA Western analysis were performed. Again, ubiquitin-conjugated BCL-3 adducts were detected when BCL-3 and GSK3 were coexpressed (Figure 3D, upper panel, compare lanes 1 and 4), and LiCl treatment decreased

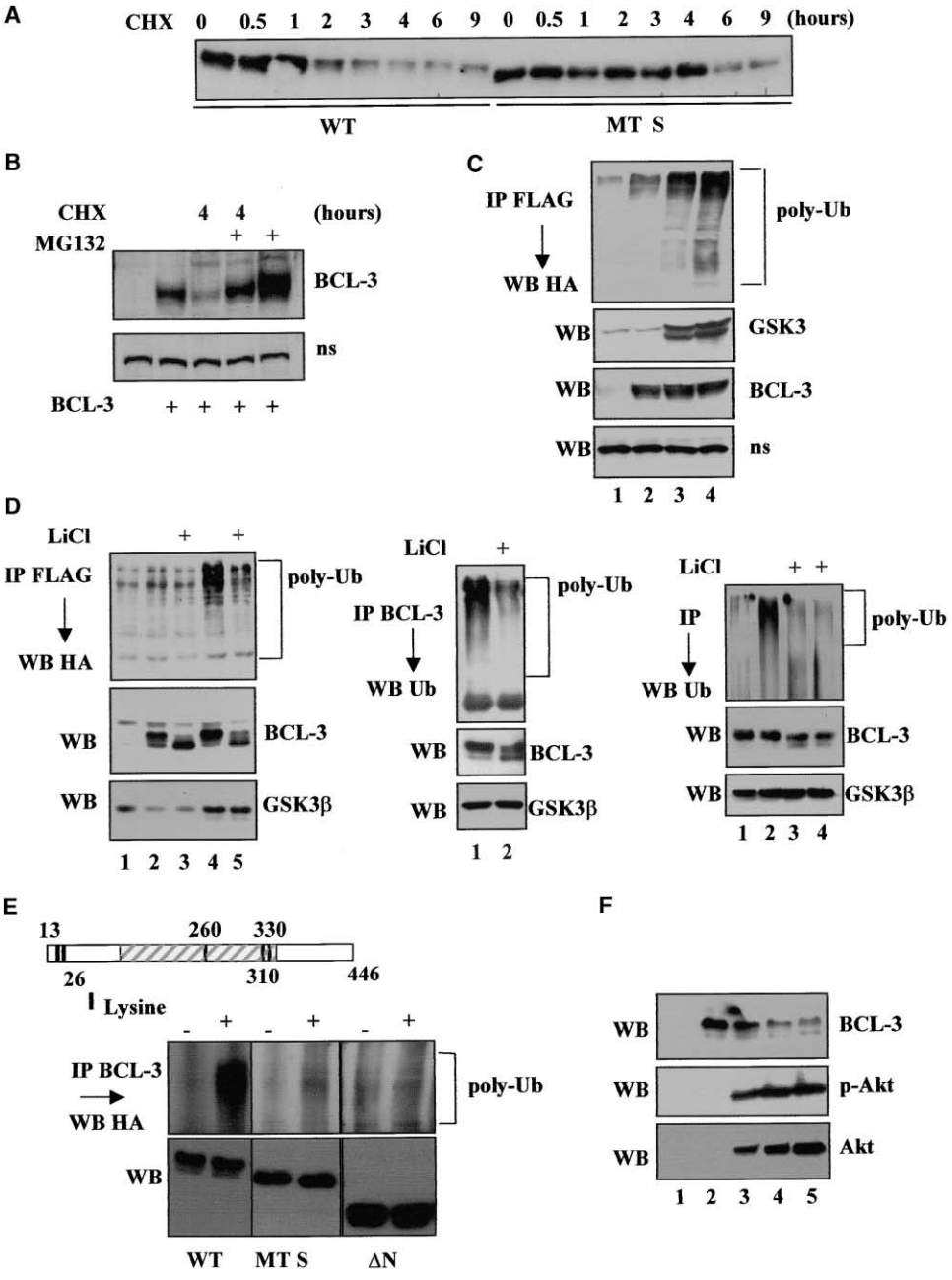


Figure 3. GSK3-Mediated BCL-3 Phosphorylation and Subsequent Degradation through Ubiquitin Linkage Is Inhibited by Akt

(A) The BCL-3 MT S is more stable than the wild-type BCL-3 protein. 293 cells transfected with either the wild-type BCL-3 or BCL-3 MT S expression plasmid were treated with 50 μg/ml cycloheximide ("CHX") for the indicated times. An anti-BCL-3 Western blot was carried out on the resulting extracts.

(B) BCL-3 degradation occurs through the proteasome pathway. 293 cells were transfected either with pcDNA3 (first lane) or with a BCL-3 expression vector (other lanes, as indicated). Cells were left unstimulated (second lane) or treated with CHX for 4 hr (third lane) or with MG132 for 30 min followed by CHX for 4 hr (fourth lane) or with MG132 alone for 4 hr (fifth lane), as indicated. An anti-BCL-3 Western blot (upper panel) was carried out on the extracts. A nonspecific signal of the anti-BCL-3 Western blot ("ns") was used for normalization.

(C) GSK3 triggers BCL-3 ubiquitin linkage. 293 cells were transfected either with HA-ubiquitin alone (lane 1) or with both HA-ubiquitin and FLAG-BCL-3 (lane 2) or with a combination of HA-ubiquitin, FLAG-BCL-3, and increasing amounts of GSK3β (lanes 3 and 4). Cells were treated for 90 min with MG132 prior to cell lysis, and anti-FLAG imunoprecipitations followed by anti-HA Western analysis were carried out on the extracts (top panel). Anti-GSK3 and -BCL-3 Western blots were performed on the cell extracts as well (bottom panels), and a nonspecific signal of the anti-BCL-3 Western blot ("ns") was used for normalization.

(D) GSK3-mediated BCL-3 ubiquitination is inhibited by LiCl treatment in 293 cells, BCL-3-expressing MEFs, and Karpas cells (left, middle, and right panels, respectively). On the left, 293 cells were transfected with HA-ubiquitin alone (lane 1) or with both HA-ubiquitin and FLAG-BCL-3 (lanes 2 and 3) or with a combination of HA-ubiquitin, FLAG-BCL-3, and GSK3β (lanes 4 and 5). Cells were left unstimulated (lanes 1, 2, and 4) or treated with LiCl 50 mM for 2 hr (lanes 3 and 5) followed by a 2 hr treatment with MG132 (lanes 1–5). Anti-FLAG immunoprecipitations followed by anti-HA Western analysis were carried out on the cell extracts. Anti-FLAG and anti-GSK3 Western blots were performed on the cell extracts.

BCL-3 ubiquitination (Figure 3D, upper panel, compare lanes 4 and 5). A slight decrease of BCL-3 ubiquitination was also detected after LiCl treatment in the absence of GSK3 overexpression (Figure 3D, upper panel, compare lanes 2 and 3). An anti-BCL-3 Western blot on the extracts again showed decreased BCL-3 phosphorylation in the presence of LiCl (Figure 3D, middle panel, compare lane 2 with lane 3 and lane 4 with lane 5). We next investigated the effect of LiCl in MEF cells infected with a retroviral vector expressing BCL-3 and in Karpas cells (Figure 3D, middle and right panels, respectively) and also observed that this GSK3 inhibitor led to a decrease of BCL-3 ubiquitination (Figure 3D, in the middle, upper panel, lane 2, and on the right, upper panel, compare lanes 3 and 4 with lane 2). Therefore, LiCl decreased BCL-3 ubiquitination through inhibition of GSK3 in a variety of cellular models.

BCL-3 harbors five lysine residues: two, K13 and K26, in the N-terminal domain and three, K260, K310, and K330, within the ankyrin repeats (Figure 3E). To determine which residues are targeted for ubiquitination and subsequent BCL-3 degradation, wild-type BCL-3, BCL-3 MT S, or a BCL-3 mutant lacking the N-terminal 118 amino acids (ΔN BCL-3) was expressed in 293 cells together with an HA-ubiquitin expression plasmid (Figure 3E, "+" lanes). ΔN BCL-3 was reproducibly expressed at higher levels compared to wild-type BCL-3 but showed the same phosphorylation profile (Figure 3E, lower panels). Anti-BCL-3 immunoprecipitations followed by anti-HA Western blots showed BCL-3 polyubiquitination when both HA-Ub and wild-type BCL-3 were coexpressed (Figure 3E, "+" lanes). Polyubiquitination was barely detectable with the BCL-3 MT S and was not detected after ΔN BCL-3 expression (Figure 3E, upper panels). These results suggest that GSK3-mediated BCL-3 phosphorylation triggers its subsequent degradation through ubiquitin linkage on N-terminal lysine residues, presumably K13 and K26.

As GSK3 activation is inhibited by the Akt/PKB kinase (Cross et al., 1995), we investigated BCL-3 phosphorylation in 293 cells transfected with a retroviral construct expressing BCL-3-IRES-GFP with or without increasing amounts of a constitutively activated Akt (Myr-Akt; Figure 3F, lanes 2–5). Overexpression of Myr-Akt led to a decrease of BCL-3 phosphorylation (Figure 3F, upper panel, compare lane 2 with lanes 3–5), whereas the BCL-3 hypophosphorylated forms slightly increased. GFP expression remained unchanged (data not shown). Therefore, Akt activation prevents BCL-3 phosphorylation, presumably through GSK3 inhibition.

### GSK3-Mediated BCL-3 Phosphorylation Does Not Affect Its Interaction with p50 and p52

As BCL-3 controls transcription through formation of heterocomplexes with p50 or p52 (Bours et al., 1993: Franzoso et al., 1993; Fujita et al., 1993), we investigated whether GSK3 regulates BCL-3's ability to bind these proteins and activate transcription from a κB site. EMSA experiments were carried out with nuclear extracts from 293 cells transfected with p52 either alone or in combination with wild-type BCL-3, BCL-3 MT S, or BCL-3 MT K, a BCL-3 mutant with both lysines 13 and 26 mutated to arginines. An NF-κB binding activity was detected in cells transfected with p52 alone, and this activity was enhanced in a similar way in the presence of wild-type and mutant BCL-3 proteins (Figure 4A). Therefore, GSK3-mediated phosphorylation does not appear to regulate the ability of the BCL-3/p52 heterocomplex to bind DNA.

The transactivation potential of BCL-3 and its mutants was investigated by performing luciferase assays, using a κB reporter plasmid. When expressed alone, wild-type BCL-3 as well as BCL-3 MT S and MT K barely induced the luciferase activity, which was, however, strongly enhanced when p52 was coexpressed (Figure 4B, left panel). Interestingly, the BCL-3 MT K/p52 complex systematically displayed reduced transactivation abilities compared to wild-type BCL-3 and BCL-3 MT S/p52 complexes (Figure 4B). The wild-type BCL-3/p50 complexes transactivated less efficiently than the BCL-3/p52 complexes, and this transactivation was not reduced with the BCL-3 MT S and MT K mutants (Figure 4B, right panel). We next investigated whether BCL-3 phosphorylation regulated its ability to interact with p50 or p52. Extracts from 293 cells transfected with a p50 or p52 expression plasmid in combination with wild-type BCL-3, BCL-3 MT S, or BCL-3 MT K vectors were immunoprecipitated with anti-BCL-3 or HA (negative control) antibodies, and anti-p50 or -p52 Western blots were performed on the immunoprecipitates (Figures 4C and 4D). In these conditions, p50 and p52 interacted with BCL-3 independently of the presence of the GSK3 phosphorylation sites and of the lysine residues (Figures 4C and 4D, upper panels). Taken together, these results demonstrate that BCL-3's ability to interact with p50 and p52 is not modulated by GSK3-mediated phosphorylation.

### BCL-3 Interacts with HDAC1, -3, and -6

We previously demonstrated that IκBα interacts with HDAC1 and -3, but not with HDAC2, -4, -5, and -6 (Via-

In the middle, BCL-3-expressing MEF cell extracts were subjected to anti-BCL-3 immunoprecipitations followed by anti-ubiquitin Western analysis (top panel). Anti-BCL-3 and GSK3β Western analysis on the cell extracts are shown (bottom panels). On the right, Karpas cells were left unstimulated (lanes 1 and 2) or treated for 2 or 6 hr with LiCl (lanes 3 and 4, respectively) followed by a 2 hr treatment with MG132 (lanes 1–4). Cell extracts were subjected to an immunoprecipitation using either a preimmune serum (negative control, lane 1) or an anti-BCL-3 antibody (lanes 2–4) followed by an anti-Ub Western blot (upper panel). Extracts were subjected to anti-GSK3β and BCL-3 Western analysis as well.

(E) Ubiquitination of wild-type BCL-3, but not BCL-3 mutants. Representation of the BCL-3 protein on the top. The ankyrin repeats are shown as a hatched rectangle, whereas the lysine residues are represented by vertical bars. On the bottom, 293 cells were transfected with vectors for wild-type BCL-3, BCL-3 MT S, or ΔN-BCL-3 alone (−) or combination with HA-ubiquitin (+), and anti-BCL-3 immunoprecipitation experiments followed by anti-HA Western blots were done on the extracts (upper panel). An anti-BCL-3 Western blot is illustrated at the bottom panel.

(F) Constitutively activated Akt inhibits constitutive BCL-3 phosphorylation. 293 cells were transfected with pcDNA3 (lane 1) or with a BCL-3-IRES-GFP-expressing construct with or without (lane 2) increasing amounts of constitutively activated Akt (Myr-Akt, lanes 3–5). Anti-BCL-3, anti-Akt, and anti-phospho Akt Western analyses were carried out on the extracts.

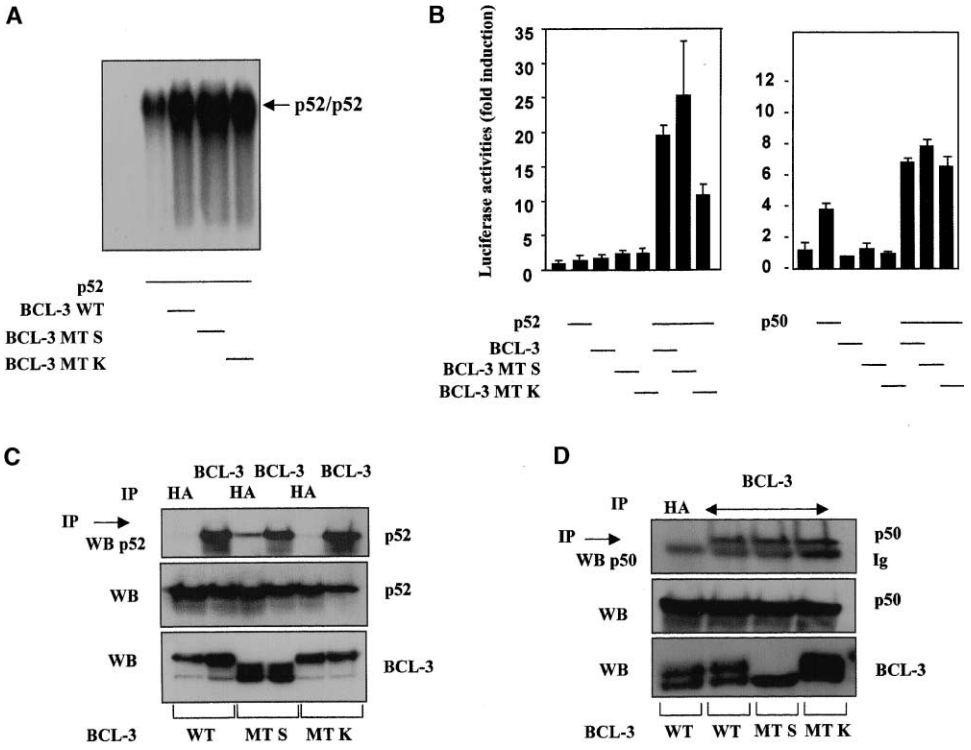


Figure 4. BCL-3 Phosphorylation Does Not Affect DNA Binding, Transcriptional Activity, and Interaction with p50 and p52

(A) p52 enhanced DNA binding activities by wild-type and BCL-3 mutants. 293 cells were transfected with either pcDNA3, p52, or with a combination of p52 and wild-type BCL-3, BCL-3 MT S, or BCL-3 MT K. EMSA were performed with the resulting nuclear extracts and a κB probe.

(B) Transcription potential of the wild-type and BCL-3 mutants on a κB reporter plasmid. 293 cells were transfected with 0.2 μg of RSV-βgal and 0.5 μg of the κB reporter plasmid either alone or with 0.5 μg of the indicated expression plasmid, and luciferase activities were measured. The data from three independent experiments performed in triplicate after normalization with the β-galactosidase activities of the extracts are shown (mean values ± SD).

(C and D) BCL-3 and its mutants interact in a similar way with p52 (C) or p50 (D). 293 cells were transfected with p52 (C) or p50 (D) and wild-type BCL-3, BCL-3 MT S, or BCL-3 MT K, and anti-BCL-3 or -HA (negative control) immunoprecipitations followed by anti-p52 (C) or p50 (D) Western blots (upper panels) were performed. The presence of p52, p50, and wild-type BCL-3 and mutants in the extracts is illustrated by Western analysis (middle and lower panels).

tour et al., 2003b). As this interaction requires IκBα ankyrin repeats, we determined whether BCL-3 also interacts with the HDAC proteins by detecting ectopicaly expressed BCL-3 in the anti-FLAG immunoprecipitates of cells transfected with BCL-3 and the FLAG-tagged HDAC vectors. BCL-3 associated with HDAC1 (Figure 5A, left and top panel, lane 2), HDAC3, and HDAC 6 (Figure 5A, top panel on the right, lanes 2 and 8, respectively), but not with HDAC2 (Figure 5A, left and top panel, lane 4), -4, and -5 (Figure 5A, top panel on the right, lanes 4 and 6, respectively).

To investigate whether GSK3-mediated BCL-3 phosphorylation regulates its interaction with these transcriptional repressors, FLAG-HDAC1 was cotransfected with wild-type, BCL-3 MT S, or BCL-3 MT K expression vectors, and anti-BCL-3 (or anti-HA as negative controls) immunoprecipitations were performed prior to anti-FLAG Western blots on the immunoprecipitates. All three BCL-3 proteins associated with HDAC1 in a similar manner (Figure 5B, top panel). The reverse immunoprecipitation was carried out by detecting BCL-3 in the anti-FLAG immunoprecipitates. As expected, HDAC1 associated with all three BCL-3 proteins (Figure 5C, left and top panels, lanes 2, 4, and 6). While the hyperphosphorylated forms of wild-type BCL-3 and BCL-3 MT K were predominant in the input, BCL-3 proteins in the immunoprecipitates showed predominantly the hypophosphorylated forms (Figure 5C, left and top panels, compare lanes 2, 4, and 6 with the lower panel showing BCL-3 expression in the input). A similar observation was also made for HDAC3 and HDAC6 (Figure 5C, middle and right panels on the top, respectively). Therefore, these results suggest that GSK3-mediated BCL-3 phosphorylation modulates BCL-3 interaction with a subset of HDAC proteins.

### GSK3-Mediated BCL-3 Phosphorylation on S394/S398 Attenuates Its Oncogenicity

As BCL-3 overexpression has been associated with B cell chronic lymphocytic leukaemia and because BCL-3 is phosphorylated in lymphoma cells, we investigated whether BCL-3's transforming properties are regulated by GSK3-mediated phosphorylation. NIH3T3 cells stably expressing the different BCL-3 forms were generated by infection with either an empty retroviral vector (negative control) or a retroviral construct expressing wild-type BCL-3, MT S, MT K, or RasV12 (positive control). Cells infected with the empty vector did not express BCL-3,

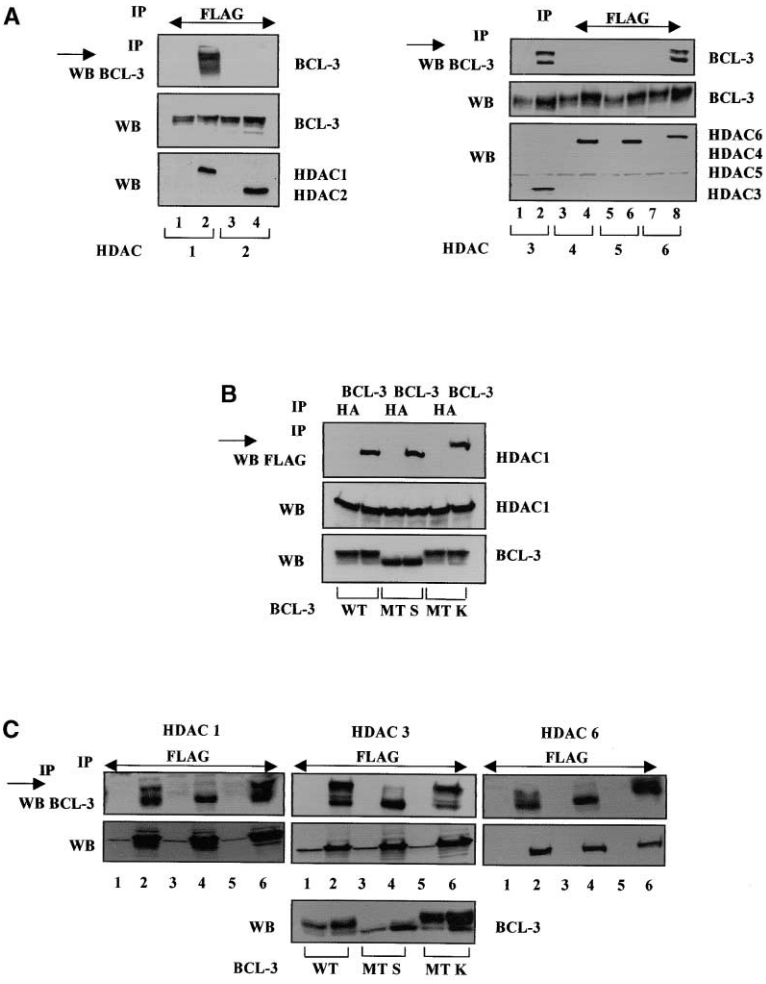


Figure 5. BCL-3 Interacts with HDAC1, -3, and -6

(A) BCL-3 interacts with HDAC1, -3, and -6, but not with HDAC2, -4, and -5. 293 cells were transfected with a BCL-3 expression vector either alone (left and right panels, odd lanes) or together with FLAG-tagged HDAC1, -2 (left panels, even lanes), -3, -4, -5, or -6 (right panels, even lanes) vectors, and anti-FLAG immunoprecipitations followed by anti-BCL-3 Western analysis were performed on the cell extracts (upper panels). The presence of BCL-3 and FLAG-tagged HDAC proteins in the cell extracts is illustrated by Western analysis using the corresponding antibodies (middle and lower panels).

(B) BCL-3 and its mutants interact with HDAC1. 293 cells were transfected with vectors for FLAG-HDAC1 and wild-type BCL-3, BCL-3 MT S, or BCL-3 MT K. Anti-BCL3 or anti-HA (negative control) immunoprecipitations followed by anti-FLAG Western blots were done on the extracts (upper panel). The presence of BCL-3 and FLAG-tagged HDAC1 in the cell extracts is illustrated by Western blots using the corresponding antibodies (lower and middle panels).

(C) Hypophosphorylated forms of BCL-3 preferentially interact with HDAC1, -3, and -6. 293 cells were transfected with FLAG-HDAC1, -3, or -6 (left, middle and right panels, respectively) and wild-type BCL-3 (lanes 1 and 2), BCL-3 MT S (lanes 3 and 4), or BCL-3 MT K (lanes 5 and 6) expression vectors, and anti-FLAG immunoprecipitations were carried out followed by anti-BCL-3 Western analysis on the cell extracts (upper panels). An anti-BCL-3 Western blot performed on the cell lysates is shown (lower panel). The presence of HDAC1, -3, and -6 is illustrated by Western analysis performed with anti-HDAC1, -3, or FLAG antibodies, respectively (middle panels).

while the cells infected with the BCL-3 retroviral constructs did (Figure 6A).

The proliferation of the NIH3T3 cells expressing BCL-3 or its mutant forms was evaluated. Wild-type BCL-3-expressing cells proliferated slightly faster than the cells infected with the empty vector or the BCL-3 MT K, while the proliferation rate of the BCL-3 MT S cells turned out to be significantly higher (Figure 6B). Therefore, BCL-3 overexpression enhances NIH3T3 proliferation, and GSK3-mediated phosphorylation attenuates this effect.

The BCL-3 oncogenicity in NIH3T3 cells was further assessed in vitro by foci formation assays. Cells infected with an empty vector developed only a few isolated foci, while wild-type BCL-3-expressing cells generated a high number of them (Figure 6C). Strikingly, foci number was further increased in BCL-3 MT S-expressing cells. Foci were not more numerous in BCL-3 MT K-expressing cells, but their size was increased compared to wild-type BCL-3-expressing cells (Figure 6C).

The same infected NIH3T3 cells were injected in the flank of nude mice, and tumor development was monitored for 3 weeks (Figure 6D). Injection of RasV12-expressing cells led to massive tumor development as expected. While none of the negative control cells generated tumors, two out of eight mice injected with wild-type BCL-3-expressing cells had significant tumor formation. While that ratio was not significantly different in mice injected with BCL-3 MT K-expressing cells (three out of eight), six out of eight mice injected with BCL-3 MT S-expressing cells developed tumors. These results show that BCL-3 is able to induce tumor growth in vivo. Moreover, this oncogenic potential was enhanced by mutations of the GSK3 phosphorylation sites.

### GSK3-Dependent BCL-3 Phosphorylation Regulates the Expression of Some BCL-3 Target Genes

As mutation of both GSK3 phosphorylation sites enhanced BCL-3 oncogenicity, we performed microarray analysis in order to identify genes differentially regulated by wild-type BCL-3 versus BCL-3 MT S and BCL-3 MT K. Total RNAs extracted from NIH3T3 cells stably infected with either an empty retroviral vector, the wild-type BCL-3, BCL-3 MT S, or BCL-3 MT K mutants were submitted to microarray analysis. The transcription of as many as 50 genes were induced in NIH3T3 cells overexpressing BCL-3 by comparison with control cells. Surprisingly, despite a more pronounced oncogenic potential, BCL-3 MT S regulated most of these target genes similarly compared to wild-type BCL-3. Only four of these genes showed different regulation between wild-

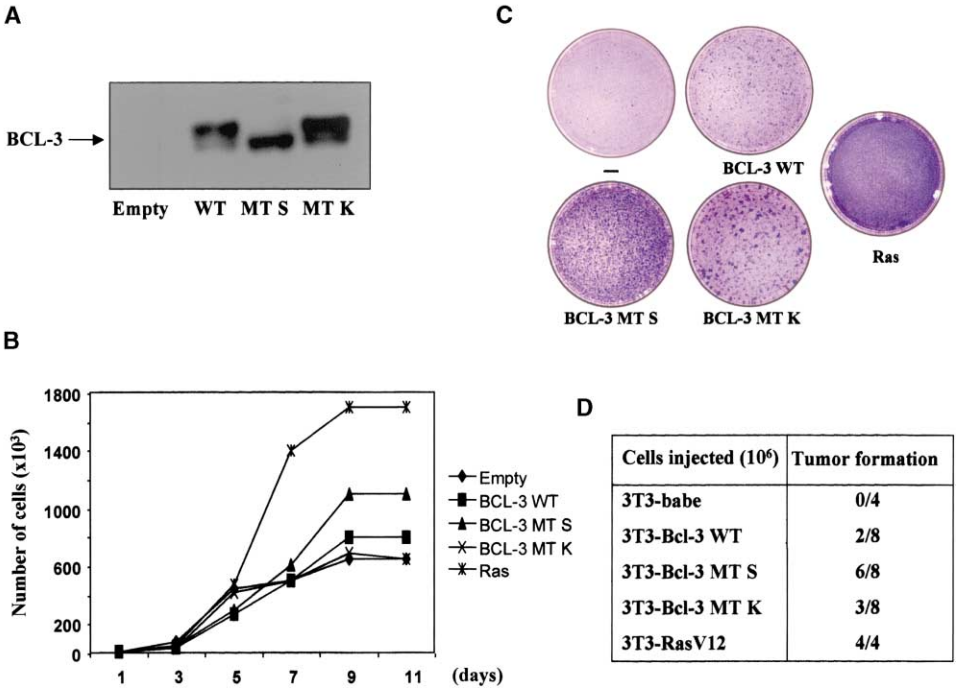


D

| Cells injected ($10^6$) | Tumor formation |
|---|---|
| 3T3-babe | 0/4 |
| 3T3-Bcl-3 WT | 2/8 |
| 3T3-Bcl-3 MT S | 6/8 |
| 3T3-Bcl-3 MT K | 3/8 |
| 3T3-RasV12 | 4/4 |

Figure 6. BCL-3 and Its Mutants Are Oncogenic In Vitro and In Vivo

(A) Expression of wild-type BCL-3, BCL-3 MT S, and BCL-3 MT K in NIH3T3 infected with the corresponding retroviral constructs.

(B) BCL-3 MT S has an enhanced proliferative phenotype compared to wild-type BCL-3, BCL-3 MT K, and cells infected with the empty vector. A growth curve was established for NIH3T3 cells infected with the indicated retroviral construct by counting the number of cells every 2 days for 11 days.

(C) Foci formation assays with NIH3T3 cells infected with the empty vector (top dish on the left) or with the BCL-3 vector or its mutants, as indicated. Cells infected with RasV12 were used as a positive control to visualize the foci formation after coloration with Giemsa.

(D) Wild-type BCL-3 and its mutant are oncogenic in vivo. NIH3T3 cells infected with the indicated retroviral constructs were subcutaneously injected in nude mice. Tumor formation was evaluated for three weeks after the injection.

type and BCL-3 MT S-expressing cells: *SLPI* (2-fold induction in MT S cells), Cxcl1 (2-fold induction in MT S cells), IFI205 (2.3-fold induction in MT S cells), and *CYPIBI* (2-fold repression in MT S cells). Real-time PCR experiments confirmed this expression profile in wild-type and MT S cells (Figure 7B, upper panels). On the other hand, BCL-3 MT K expression modified the expression of only 13 genes compared to control cells, suggesting that lysines 13 and 26 are critical for BCL-3 transactivation potential. The expression of these 13 candidates, namely the genes coding for pleiotrophin, Serpin B1A, collagen 5A1, IdB2, BmP1, Actin, Tbx14, Cyclin G2, Ppic 1, collagen 8A1, and Rgs 16, is regulated by wild-type BCL-3, and mutants and can thus be considered sufficient to induce cell transformation (Figure 7A). The expression profile of three of these genes (*pleiotrophin*, *serpin B1A*, and *IdB2*) was also confirmed by real-time PCR experiments (Figure 7B, lower panels).

## Discussion

In this report, we identified GSK3 as a BCL-3 kinase and demonstrated that this phosphorylation critically modulates BCL-3 function by triggering its degradation by modulating its oncogenicity and by selectively regulating a subset of newly identified BCL-3 target genes. We provided several lines of evidence for BCL-3 being a new GSK3 substrate. First, BCL-3 is phosphorylated by this kinase in vitro on GSK3 consensus residues. While most GSK3 substrates require a primo phosphorylation, we could not identify any priming kinase for BCL-3. Indeed, CKII, which often acts as the priming kinase, does not phosphorylate BCL-3. However, previous work showed that this primo phosphorylation is dispensable when a proline residue is present downstream of the targeted residues and when GSK3 interacts with its substrate, as this is the case for BCL-3. As additional evidence for GSK3 acting as a BCL-3 kinase, LiCl, a specific GSK3 inhibitor, prevents constitutive BCL-3 phosphorylation and subsequent ubiquitination in a variety of cellular models including 293 cells, MEFs, and Karpas cells. Interestingly, mutation of both GSK3 phosphorylation sites completely abolished constitutive BCL-3 phosphorylation, therefore indicating that GSK3 is the main kinase that constitutively phosphorylates BCL-3. We also show that endogenous GSK3$\alpha$, but not GSK3$\beta$, interacts with BCL-3, which does not rule out the possibility that both kinases phosphorylate BCL-3 in vivo. In any case, GSK3$\alpha$ can compensate the loss of GSK3$\beta$ for BCL-3 phosphorylation since this oncoprotein was still constitutively phosphorylated in MEF cells KO for GSK3$\beta$ (data not shown).

GSK3-mediated BCL-3 phosphorylation is constitutive and targets its subsequent degradation through ubi-

**A**

| Empty versus | Bcl-3 WT | | MT S | | MT K | |
|---|---|---|---|---|---|---|
| Pleiotrophin | 14.82 | *(0.00002)* | 8.57 | *(0.000023)* | 6.36 | *(0.000189)* |
| SerpinB1A | 22.62 | *(0.00002)* | 34.29 | *(0.00002)* | 2.29 | *(0.00006)* |
| Collagen5A1 | 4.28 | *(0.00002)* | 4.9 | *(0.00002)* | 2 | *(0.001077)* |
| Idb2 | 4.9 | *(0.000023)* | 4 | *(0.00004)* | 2.82 | *(0.000307)* |
| Bmp1 | 2.82 | *(0.004481)* | 2.46 | *(0.000307)* | 2.29 | *(0.000865)* |
| Actin, a | 2.46 | *(0.00002)* | 2.46 | *(0.00006)* | 2 | *(0.000273)* |
| Tbx14 | 2.63 | *(0.002753)* | 1.14 | *NC* | 5.27 | *(0.001336)* |
| CyclinG2 | 2 | *(0.000167)* | 2.29 | *(0.00929)* | 2.63 | *(0,000346)* |
| SLPI | 6.06 | *(0.00002)* | 11.31 | *(0.00002)* | 1.4 | *NC* |
| Ppic1 | 0.4 | *(0.99998)* | 0.574 | *(0.99998)* | 0.4 | *(0.99998)* |
| Collagen8A1 | 0.04 | *(0.999886)* | 0.038 | *(0.998923)* | 0.28 | *(0.999759)* |
| Cxcl1 | 0.25 | *(0.99998)* | 0.5 | *(0.99998)* | 0.4 | *(0.99998)* |
| Rgs16 | 0.033 | *(0.998514)* | 0.0625 | *(0.99987)* | 0.038 | *(0.999135)* |

**B**

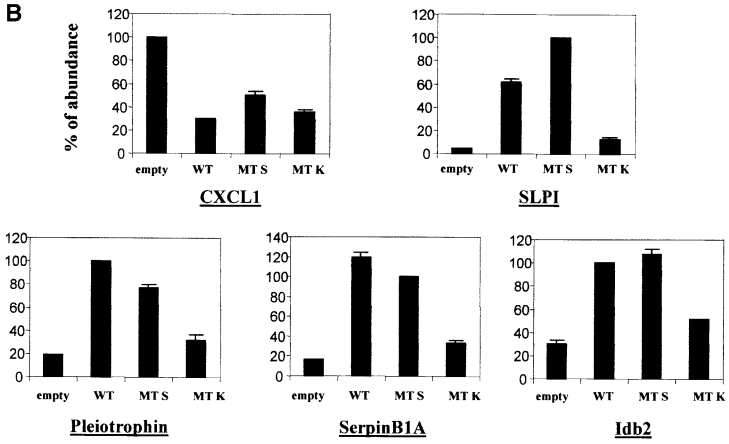


Figure 7. Phosphorylation-Dependent Regulation of a Subset of Newly Identified BCL-3 Target Genes

(A) Microarray analyses were carried out using RNAs extracted from NIH3T3 cells infected with the indicated retroviral constructs. The identity of the BCL-3 target genes as well as the intensity of their induction or their repression in the BCL-3 expressing cells (fold induction) and the p values are mentioned. The level of expression in control cells is set to 1.

(B) Expression of selected BCL-3 target genes. RNA was extracted from infected NIH3T3 cells, and gene expression was measured by real-time PCR. The transcript copy number for the most abundant population is set to 100%. Control corresponds to the NIH3T3 cells stably infected with the empty retroviral construct, whereas "WT," "MT S," and "MT K" correspond to the NIH3T3 cells stably infected with the wild-type, the MT S, or the MT K BCL-3 expressing retrovirus, respectively. The data were normalized by quantification of the GAPDH transcripts.

quitin linkage and proteasome decay. GSK3-mediated substrate degradation (Frame and Cohen, 2001) has already been described for cyclin D1 (Diehl et al., 1998) and cyclin E (Welcker et al., 2003). As BCL-3 is oncogenic, this mechanism may represent a way to control BCL-3 levels in normal cells. Any translocation that causes BCL-3 overexpression may then overcome GSK3-mediated BCL-3 phosphorylation and degradation.

BCL-3 has been described as a transcriptional activator (Bours et al., 1993; Fujita et al., 1993). Therefore, BCL-3 presumably recruits coactivator complexes and/or removes corepressors such as the HDAC proteins from the promoter vicinity to activate transcription (Baek et al., 2002). We identified three HDAC proteins, namely HDAC1, -3, and -6, that interact with BCL-3. Although both hypophosphorylated and phosphorylated forms of BCL-3 were found associated with the HDAC proteins, we noticed that hypophosphorylated BCL-3 preferentially interacted with the HDACs. As BCL-3 has been described as a transcriptional activator (Bours et al., 1993), the hypophosphorylated forms of BCL-3 could more efficiently remove corepressors such as the HDAC proteins from the promoters and therefore better activate some target genes expression. Our microarray analysis is in favor of this hypothesis, at least for some BCL-3 target genes such as *SLPI* (see below).

We noticed that the BCL-3 MT K that is no longer ubiquitinated had a decreased transactivation effect. Interestingly, both targeted lysine residues are within one BCL-3 transactivation domain (Bours et al., 1993). Several studies demonstrated that some DNA-bound transactivation factors are targeted for ubiquitination within their transactivation domain and this signal is required for transcriptional activation (Conaway et al., 2002; Freiman and Tjian, 2003). Therefore, there may be a link between BCL-3 ubiquitination and activation. Alternatively, the same lysine residues could also be targeted for acetylation, a posttranslational modification associated with transcriptional activation (Freiman and Tjian, 2003), although we have no evidence for BCL-3 being acetylated so far (data not shown). In any case, both lysine residues appear to be critical for optimal BCL-3 mediated transcription since many BCL-3 target genes that we identified here (see below) were not induced in NIH3T3 cells overexpressing the BCL-3 MT K.

This paper demonstrates that BCL-3 can directly transform cells in vitro. By comparing transformation by wild-type and mutated BCL-3, we observed that all three

forms are transforming, but mutation of S394 and S398 significantly enhanced BCL-3 oncogenic potential. The role of GSK3 in the modulation of BCL-3 oncogenicity is strongly suggested by our data since we show that GSK3 is the main BCL-3 kinase and phosphorylates this oncoprotein in various cell types including the karpas cells, which are derived from an anaplastic large cell lymphoma. Because we also show that Akt inhibits BCL-3 phosphorylation, it is tempting to speculate that constitutive Akt activation, a hallmark of many transformed cells, attenuates BCL-3 phosphorylation and its subsequent degradation, thus enhancing BCL-3 oncogenicity.

Very few BCL-3 target genes have been characterized so far (Westerheide et al., 2001; Elliott et al., 2002). We identified fifty new BCL-3 target genes. Many of them are known to play critical roles in oncogenesis, and some of them have already been described as NF-κB target genes (data not shown). Most of the identified BCL-3 target genes were similarly induced in cells infected with wild-type or MT S BCL-3, indicating that GSK3-mediated BCL-3 phosphorylation does not modulate the expression of most of its target genes. A few target genes are however sensitive to BCL-3 phosphorylation and include *SLPI* (Devoogdt et al., 2003), *Cxcl1*, *CYPIBI*, and *IFI205*. *SLPI* has already been described as an NF-κB target gene in pre-B cells, but its expression is decreased by NF-κB (Li et al., 2001). *SLPI* is strongly induced in BCL-3-overexpressing cells, and its level of expression is further enhanced in cells overexpressing BCL-3 MT S. Therefore, it is tempting to speculate that *SLPI* overexpression participates in BCL-3 oncogenicity. Indeed, *SLPI* promotes in vivo tumor formation by Lewis lung carcinoma cells (Devoogdt et al., 2003). *Cxcl1* has also been described as an NF-κB target gene in melanoma cells (Wood and Richmond, 1995). As BCL-3 modifies *Cxcl1* expression, multiple NF-κB proteins can possibly transactivate this target gene.

In conclusion, our data indicate that GSK3 constitutively phosphorylates BCL-3 and triggers its degradation. This phosphorylation limits BCL-3 oncogenicity, probably by reducing BCL-3 lifespan and by limiting the transcription of a subset of BCL-3 target genes.

## Experimental Procedures

### Cell Culture, Biological Reagents, and Treatments

MEFs, 293, and NIH3T3 cells were maintained in DMEM supplemented with 10% fetal calf serum (Life Technologies, Grand Island, NY) and antibiotics. The Karpas 299 cell line was a gift from Dr. F. Lambert (Laboratory of Human Genetics, University of Liege, Belgium) and was cultured in RPMI supplemented with 10% fetal calf serum and antibiotics. Polyclonal anti-HA, anti-HDAC1, anti-HDAC3, anti-BCL-3, and monoclonal anti-ubiquitin antibodies were purchased from Santa Cruz Biotechnologies (Santa Cruz, CA). Anti-Akt and anti-phospho Ser 473 Akt antibodies were obtained from ICN (Costa Mesa, CA) and Cell Signaling (Beverly, MA), respectively. Anti-FLAG antibodies and beads as well as recombinant GSK3β protein were purchased from Sigma (Sigma, St Louis, MO), whereas recombinant Akt and Erk1 were obtained from Biosource (Camarillo, CA) and Calbiochem (San Diego, CA), respectively.

The FLAG-HDAC1, -2, -3, -4, -5, and -6 constructs were previously described (Viatour et al., 2003b) as were the BCL-3, p50, and p52 $pMT_2T$ expression vectors (Bours et al., 1992, 1993) and the ΔN BCL-3 $pMT_2T$ construct which lacks amino acids 1–119 of BCL-3 (Bours et al., 1993). The FLAG-tagged BCL-3 constructs were generated by PCR using the corresponding wild-type or BCL-3 mutants cloned into the pMT2T vector as templates (Bours et al., 1993). The GST-BCL-3 fusion construct was generated by subcloning the BCL-3 coding sequence into the pGEX 6P-3 plasmid (Amersham Pharmacia Biotech, Uppsala, Sweden). The wild-type BCL-3, BCL-3 MT S, and MT K coding sequences were subcloned into the pBabe puromycin retrovirus as was the wild-type BCL-3 sequence into the IRES GFP MSCV retroviral vector. The RasV12 pbabe puro was previously described (Ferbeyre et al., 2002). The GSK3β expression vector was generated by PCR amplifying and subcloning the GSK3β coding sequence from a human Marathon cDNA library (Clontech, Palo Alto, CA) into the pcDNA5 vector (Invitrogen, Carlsbad, CA). The HA-ubiquitin and Myr-Akt expression vectors were gifts from C. van Lint (Free University of Brussels, Belgium) and Y-C. Liu (LIAI, San Diego, CA), respectively.

### Bioinformatics, Kinase Assays, Site-Directed Mutagenesis, and Immunoprecipitations

Potential BCL-3 phosphoacceptor sites were searched by submitting the human BCL-3 primary amino acid sequence to the Scansite (http://scansite.mit.edu/) (Yaffe et al., 2001).

For kinase assays, GST-BCL-3 fusion protein was expressed and purified as described (Chariot et al., 1999) and incubated with a recombinant CKII kinase or increasing amounts of the recombinant GSK3β kinase for 30 min at 30°C as described (Leonardi et al., 2000).

For site mutagenesis, BCL-3 $pMT_2T$ was used as template to generate BCL-3 mutants, using the QuikChange Site-Directed Mutagenesis Kit (Stratagene, La Jolla, CA). All the BCL-3 mutants were sequenced.

Immunoprecipitations were performed as described (Viatour et al., 2003b).

### Nuclear Protein Extraction, Electrophoretic Mobility Shift Assay, and Reporter Assays

293 cells were transfected with the indicated expression vectors, and nuclear extracts as well as electrophoretic mobility shift assays (EMSA) were performed as previously described (Bentires-Alj et al., 1999). Luciferase asssays were carried out as described (Leonardi et al., 2000).

### Retroviral Transduction, Growth Curve, Foci Formation, and Nude Mice Injection

Retroviral infection of NIH3T3 cells was performed according to instructions from Dr. Nolan's laboratory (http://www.stanford.edu/group/nolan/retroviral_systems/retsys.html).

$20 \times 10^3$ cells were seeded in 12-well plates and counted every 2 days, starting 24 hr after plating. Medium was changed every 2 days. Each condition was plated and counted in triplicate. The curves show a representative experiment out of three.

For foci assays, $1.5 \times 10^6$ infected NIH3T3 cells were seeded in a 10 cm plate, and media was changed every 3 days. The cell cultures were followed for 3 weeks, and colonies were visualized with Giemsa staining.

For subcutaneous injection in nude mice, $10^6$ cells were resuspended in 200 μl of PBS and injected in the flank of 5-week-old nude mice (Swiss strain). Evaluation of tumor growth was performed twice weekly and stopped after 3 weeks when mice injected with RasV12 cells were sacrificed for ethical reasons.

### Affymetrix Microarray Analysis

Total RNAs were extracted from NIH3T3 cells stably infected with empty virus or virus expressing either wild-type BCL-3, BCL-3 MT S, or BCL-3 MT K. The integrity of the RNAs was checked using the Agilent platform (Agilent 2100 Bioanalyzer). Biotin-labeled cRNA and subsequent hybridization and scanning were performed following the manufacturer's instructions.

### Real-Time PCR

Real-time PCR was carried out using the TaqMan platform, as described (Heid et al., 1996), and primers, whose sequences are available upon request, were designed using the Primers Express software.

**Acknowledgments**

The authors are grateful to C. van Lint and Y-C. Liu for the gifts of plasmids. M.-P.M., A.C., and J.P. are Research Associates and Research Director, respectively at the Belgian National Fund for Research (F.N.R.S.). This paper is dedicated to the memory of J. Gielen. This work was supported by grants from the TELEVIE, the Centre Anti-Cancéreux, IAP5/12, and the Belgian Federation against Cancer. E.D. was supported by a grant from the Arthritis National Research Foundation (ANRF).

Received: March 31, 2004
Revised: July 14, 2004
Accepted: July 28, 2004
Published: October 8, 2004

**References**

Baek, S.H., Ohgi, K.A., Rose, D.W., Koo, E.H., Glass, C.K., and Rosenfeld, M. (2002). Exchange of N-CoR corepressor and Tip60 coactivator complexes links gene expression by NF-κB and β-amyloid precursor protein. Cell *110*, 55–67.

Ben-Neriah, Y. (2002). Regulatory functions of ubiquitination in the immune system. Nat. Immunol. *3*, 20–26.

Bentires-Alj, M., Hellin, A.C., Ameyar, M., Chouaib, S., Merville, M.P., and Bours, V. (1999). Stable inhibition of nuclear factor kappaB in cancer cells does not increase sensitivity to cytotoxic drugs. Cancer Res. *59*, 811–815.

Bours, V., Burd, P.R., Brown, K., Villalobos, J., Park, S., Ryseck, R.-P., Bravo, R., Kelly, K., and Siebenlist, U. (1992). A novel mitogen-inducible gene product related to p50/p105-NF-κB participates in transactivation through a κB site. Mol. Cell. Biol. *12*, 685–695.

Bours, V., Franzoso, G., Azarenko, V., Park, S., Kanno, T., Brown, K., and Siebenlist, U. (1993). The oncoprotein BCL-3 directly transactivates through κB motifs via association with DNA-binding p50B homodimers. Cell *72*, 729–739.

Bundy, D.L., and McKeithan, T.W. (1997). Diverse effects of BCL3 phosphorylation on its modulation of NF-κB p52 homodimer binding to DNA. J. Biol. Chem. *272*, 33132–33139.

Chariot, A., Princen, F., Gielen, J., Merville, M.-P., Franzoso, G., Brown, K., Siebenlist, U., and Bours, V. (1999). IκB-α enhances transactivation by the HOXB7 homeodomain-containing protein. J. Biol. Chem. *274*, 5318–5325.

Cogswell, P.C., Guttridge, D.C., Funkhouser, W.K., and Baldwin, A.S., Jr. (2000). Selective activation of NF-kappa B subunits in human breast cancer: potential roles for NF-kappa B2/p52 and for BCL-3. Oncogene *19*, 1123–1131.

Conaway, R.C., Brower, C.S., and Conaway, J.W. (2002). Emerging roles of ubiquitin in transcription regulation. Science *296*, 1254–1258.

Cross, D.A., Alessi, D.R., Cohen, P., Andjelkovich, M., and Hemmings, B.A. (1995). Inhibition of glycogen synthase kinase-3 by insulin mediated by protein kinase B. Nature *378*, 785–789.

Devoogdt, N., Hassanzadeh Ghassabeh, G., Zhang, J., Brys, L., De Baetselier, P., and Revets, H. (2003). Secretory leukocyte protease inhibitor promotes the tumorigenic and metastatic potential of cancer cells. Proc. Natl. Acad. Sci. USA *100*, 5778–5782.

Diehl, J.A., Cheng, M., Roussel, M.F., and Sherr, C.J. (1998). Glycogen synthase kinase-3β regulates cyclin D1 proteolysis and subcellular localization. Genes Dev. *12*, 3499–3511.

Elliott, S.F., Coon, C.I., Hays, E., Stadheim, T.A., and Vincenti, M.P. (2002). Bcl-3 is an interleukin-1-responsive gene in chondrocytes and synovial fibroblasts that activates transcription of the matrix metalloproteinase 1 gene. Arthritis Rheum. *46*, 3230–3239.

Ferbeyre, G., de Stanchina, E., Lin, A.W., Querido, E., McCurrach, M.E., Hannon, G.J., and Lowe, S.W. (2002). Oncogenic ras and p53 cooperate to induce cellular senescence. Mol. Cell. Biol. *22*, 3497–3508.

Frame, S., and Cohen, P. (2001). GSK3 takes centre stage more than 20 years after its discovery. Biochem. J. *359*, 1–16.

Franzoso, G., Bours, V., Azarenko, V., Park, S., Tomita-Yamaguchi, M., Kanno, T., Brown, K., and Siebenlist, U. (1993). The oncoprotein BCL-3 can facilitate NF-kappa B-mediated transactivation by removing inhibiting p50 homodimers from select kappa B sites. EMBO J. *12*, 3893–3901.

Freiman, R.N., and Tjian, R. (2003). Regulating the regulators: lysine modifications make their mark. Cell *112*, 11–17.

Fujita, T., Nolan, G.P., Liou, H.C., Scott, M.L., and Baltimore, D. (1993). The candidate proto-oncogene BCL-3 encodes a transcriptional coactivator that activates through NF-kappa B p50 homodimers. Genes Dev. *7*, 1354–1363.

Heid, C.A., Stevens, J., Livak, K.J., and Williams, P.M. (1996). Real time quantitative PCR. Genome Res. *6*, 986–994.

Karin, M., Cao, Y., Greten, F.R., and Li, Z.W. (2002). NF-kappaB in cancer: from innocent bystander to major culprit. Nat. Rev. Cancer *2*, 301–310.

Leonardi, A., Chariot, A., Claudio, E., Cunningham, K., and Siebenlist, U. (2000). CIKS, a connection to IκB-kinase and stress-activated protein kinase. Proc. Natl. Acad. Sci. USA *97*, 10494–10499.

Li, J., Peet, G.W., Balzarano, D., Li, X., Massa, P., Barton, R.W., and Marcu, K.B. (2001). Novel NEMO/IkappaB kinase and NF-kappa B target genes at the pre-B to immature B cell transition. J. Biol. Chem. *276*, 18579–18590.

McKeithan, T.W., Rowley, J.D., Shows, T.B., and Diaz, M.O. (1987). Cloning of the chromosome translocation breakpoint junction of the t(14;19) in chronic lymphocytic leukemia. Proc. Natl. Acad. Sci. USA *84*, 9257–9260.

Nishikori, M., Maesako, Y., Ueda, C., Kurata, M., Uchiyama, T., and Ohno, H. (2003). High-level expression of BCL3 differentiates t(2;5)(p23;q35)-positive anaplastic large cell lymphoma from Hodgkin disease. Blood *101*, 2789–2796.

Nolan, G.P., Fujita, T., Bhatia, K., Huppi, C., Liou, H.-C., Scott, M.L., and Baltimore, D. (1993). The *BCL-3* proto-oncogene encodes a nuclear IκB-like molecule that preferentially interacts with NF-κB p50 and p52 in a phosphorylation-dependent manner. Mol. Cell. Biol. *13*, 3557–3566.

Ohno, H., Takimoto, G., and McKeithan, T.W. (1990). The candidate proto-oncogene BCL-3 is related to genes implicated in cell lineage determination and cell cycle control. Cell *60*, 991–999.

Viatour, P., Bentires-Alj, M., Chariot, A., Deregowski, V., de Leval, L., Merville, M.P., and Bours, V. (2003a). NF-kappa B2/p100 induces Bcl-2 expression. Leukemia *17*, 1349–1356.

Viatour, P., Legrand-Poels, S., van Lint, C., Warnier, M., Merville, M.-P., Gielen, J., Piette, J., Bours, V., and Chariot, A. (2003b). Cytoplasmic IκBα increases NF-κB-independent transcription through binding to HDAC1 and HDAC3. J. Biol. Chem. *278*, 46541–46548.

Welcker, M., Singer, J., Loeb, K.R., Grim, J., Bloecher, A., Gurien-West, M., Clurman, B.E., and Roberts, J.M. (2003). Multisite phosphorylation by Cdk2 and GSK3 controls cyclin E degradation. Mol. Cell *12*, 381–392.

Westerheide, S.D., Mayo, M.W., Anest, V., Hanson, J.L., and Baldwin, A.S., Jr. (2001). The putative oncoprotein BCL-3 induces cyclin D1 to stimulate $G_1$ transition. Mol. Cell. Biol. *21*, 8428–8436.

Wood, L.D., and Richmond, A. (1995). Constitutive and cytokine-induced expression of the melano growth stimulatory activity/GRO alpha gene requires both NF-kappaB and novel constitutive factors. J. Biol. Chem. *270*, 30619–30626.

Yaffe, M.B., Leparc, G.G., Lai, J., Obata, T., Volinia, S., and Cantley, L.C. (2001). A motif-based profile scanning approach for genome-wide prediction of signaling pathways. Nat. Biotechnol. *19*, 348–353.